NAA-SR-8431
COPY

A MATHEMATICAL MODEL DESCRIBING THE DYNAMICS OF THE SRE CORE II

AEC Research and Development Report

ATOMICS INTERNATIONAL
A DIVISION OF NORTH AMERICAN AVIATION, INC.

Price $0.75
Available from the Office of Technical Services
Department of Commerce
Washington 25, D. C.

NAA-SR-8431
PHYSICS
32 PAGES

A MATHEMATICAL MODEL DESCRIBING THE DYNAMICS OF THE SRE CORE II

By

R. W. KEATEN
A. L. GUNBY
W. J. CARLSON

ATOMICS INTERNATIONAL

A DIVISION OF NORTH AMERICAN AVIATION, INC.
P.O. BOX 309 CANOGA PARK, CALIFORNIA

CONTRACT: AT(11-1)-GEN-8
ISSUED: SEPTEMBER 15, 1963

DISTRIBUTION

This report has been distributed according to the category "Physics" as given in "Standard Distribution Lists for Unclassified Scientific and Technical Reports" TID-4500 (21st Ed.), June 1, 1963. A total of 680 copies was printed.

ABSTRACT

A mathematical model explaining the dynamics of the SRE Core II, prior to constraint of the fuel clusters, has been developed and shown to match the measured SRE behavior. The model uses an axial space-independent, nodal approach, postulating separate coolant flow regions inside and outside the fuel cluster, plus a "mixing flow" between them. The model reproduces the power coefficient and flux oscillations by demonstrating the effect of the mixing flow on fuel-rod bowing.

CONTENTS

FIGURES

I. INTRODUCTION

The dynamics of the second core fuel loading of the SRE have been described in detail in other reports[1,2,3,4] and will be only briefly reviewed here. When the power level of the reactor was first increased to 10% of full power, accurate control became difficult. Measurements with various experimental techniques showed that the prompt power coefficient was unexpectedly positive, and that it varied with the delta T across the core as shown in Figure 1. (The moderator coefficient, which is positive, is much slower than that of the fuel channels, and is neglected throughout this paper.)

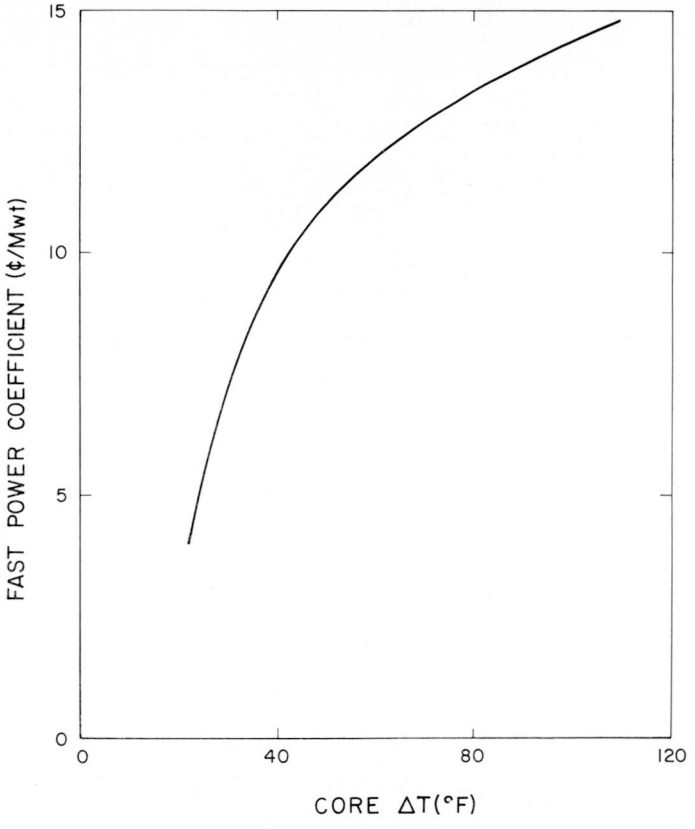

7602-5005

Figure 1. Measured Fast Power Coefficient, SRE

Outward bowing of the fuel rods was postulated as the cause of the positive prompt power coefficient. A maximum outward bowing of 0.160 in. was possible (Figure 2), and rough calculations showed that the temperature distribution

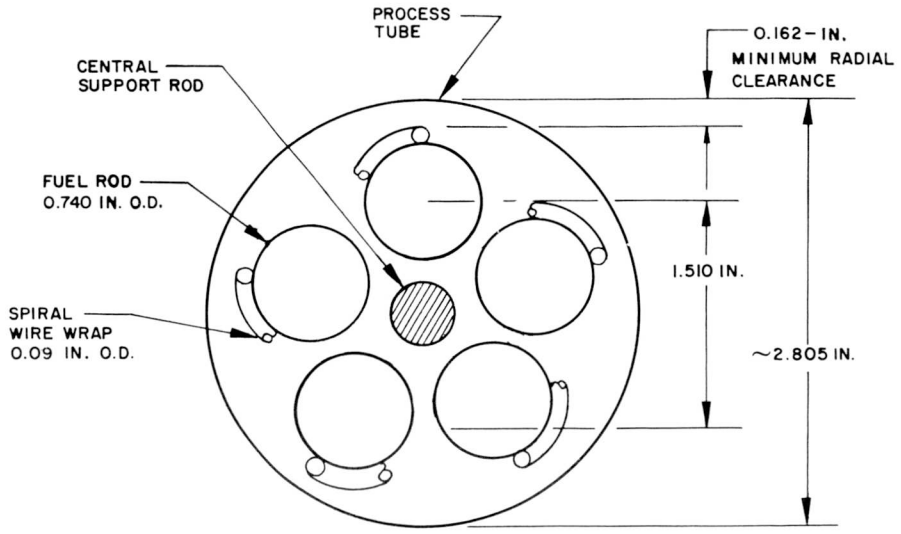

Figure 2. SRE Fuel Cluster

within the channel could cause such bowing. Measurements and calculations[5] showed that outward bowing of all the rods would increase the reactivity by 0.6 to 0.7¢ per mil of bowing of all fuel clusters. Final proof of bowing as the cause of the positive power coefficient was made by constraining the central seven clusters with a spiral wire wrap, a procedure which reduced the positive coefficient by an amount equal to the statistical weight of these clusters.

After the first seven clusters were constrained, the flux was observed to oscillate steadily with the power level constant and no control rod motion. These oscillations could not have been detected previously because of the necessity for frequent control rod motion. The amplitude and frequency of the oscillations were measured at various power levels and flow rates, and the measurements were repeated as additional clusters were wire-wrapped. As shown in Figure 3, the frequency depended only on the flow rate, while the amplitude varied with core delta T and with the number of constrained clusters. Fuel and coolant temperature oscillations of the same frequency were also observed. No particular clusters oscillated continuously; instead, they started and stopped apparently at random.

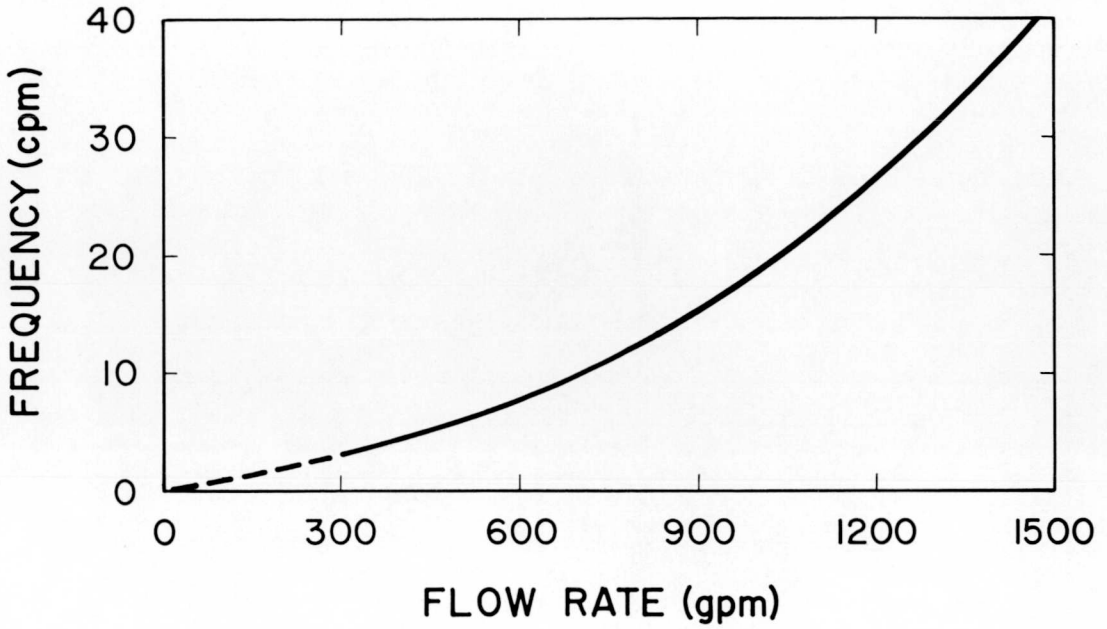

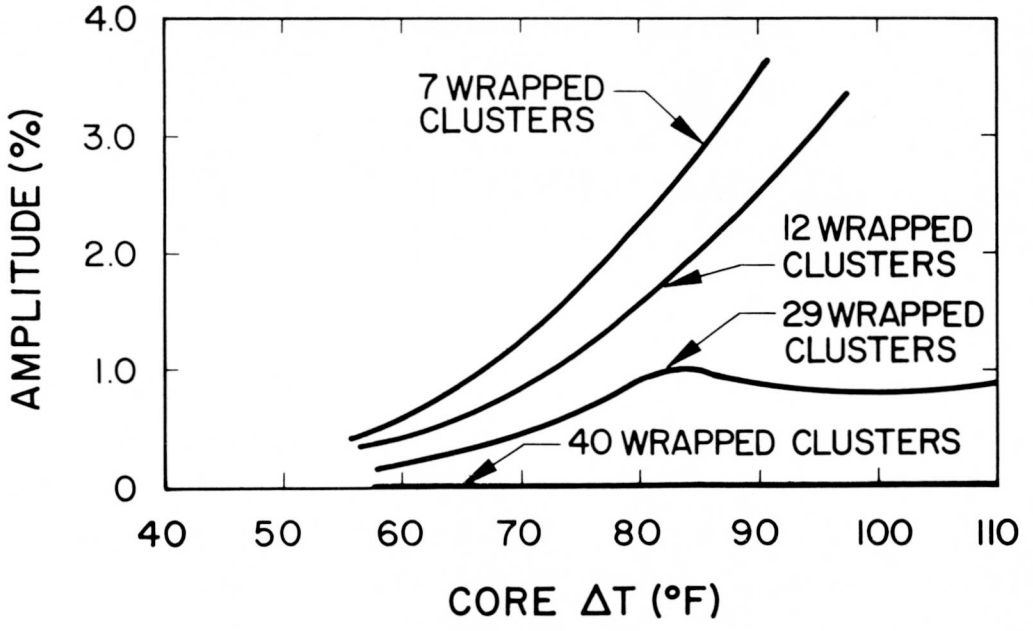

7602-5002

Figure 3. Measured Oscillations, SRE

After 12 clusters had been constrained, the controllability of the reactor improved sufficiently to permit dynamic measurements. The reactor transfer function was measured[6] at 2-1/4 Mwt by introducing a sinusoidal variation in reactivity. In Figure 4 the results are compared with those obtained at zero power. The behavior at low frequencies, where the phase angle is more

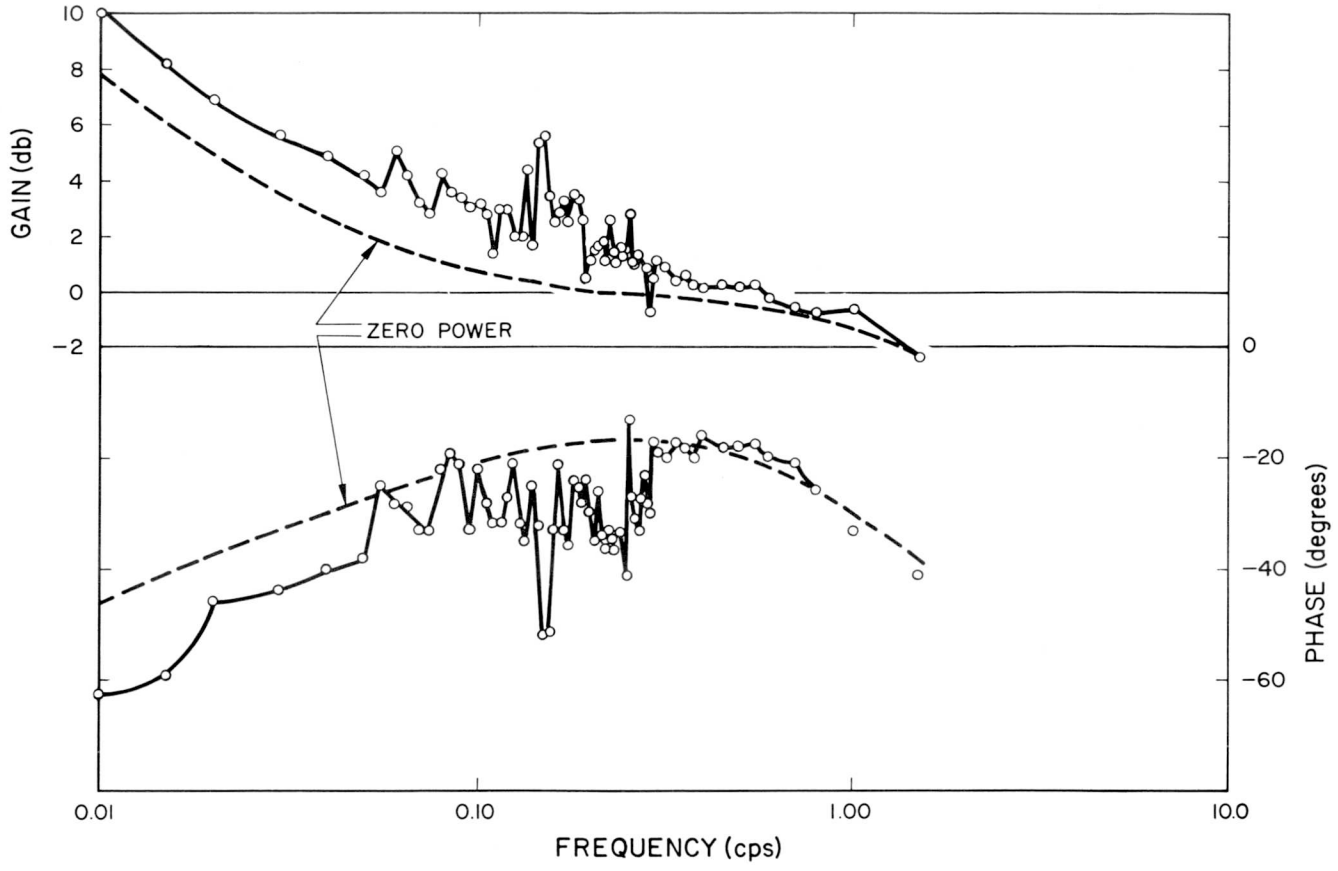

7602-5007

Figure 4. Measured Oscillations, SRE

negative than at zero power, is additional evidence of the positive fast power coefficient. The resonance structure occurs at the same frequency as the sustained flux oscillations and is thus closely related. Constraining all of the fuel clusters changed the prompt power coefficient from positive to negative, and eliminated the flux oscillations and the resonance structure in the transfer function.

Although these results conclusively demonstrated that bowing was the cause of the instability, the exact nature of the experimental results was not explained. These are: (1) the large variation in the power coefficient with power, (2) the existence and properties of flux oscillations, and (3) the nature of the transfer function. This paper presents a mathematical model of the fuel cluster and coolant which provides an explanation of these effects.

II. DESCRIPTION OF MATHEMATICAL MODEL

Fuel bowing was caused by a difference in the cladding temperature on the inside and outside of the fuel rod. For analysis of this effect, the fuel rods were divided arbitrarily into two equal sections, and each section treated as a node. Calculated and measured flux traverses show that about 75% of the power is generated in the outer section, and 25% in the inner. Heat generated at each node is transferred to the adjacent coolant, or to the other fuel node.

Hydraulic tests using a fuel cluster in a clear plastic process tube, with water as the coolant to permit visual observations, indicated three flow paths for the coolant: one inside the cluster, one outside, and a "mixing" flow between the two. An exact description of this, including spatial dependence in the axial direction as well as time variation, would become extremely complicated when coupled with all the other equations required for this model. An alternate treatment using several nodes in the axial direction with appropriate heat generation, flows, and transport delays could be constructed on an analog computer. However, a much simpler treatment, in which no axial space dependence is included, was used to determine the general behavior of the model. This model succeeded in duplicating the observed effects closely enough so that no additional complexity was needed.

As shown in Figure 2, Region 1 consists of the "outer" coolant and fuel while Region 2 contains the "inner" coolant and fuel. Therefore, the model has four nodes, two in the fuel and two in the coolant. The mixing flow between the regions is expressed as that portion, M_x, of the total coolant flow which flows between the coolant nodes. Since the fuel rods are individually wire-wrapped, mixing occurs over the entire length, reaching a maximum at the center where bowing is greatest. On a nodal basis, therefore, total mixing flow may be greater than total coolant flow since the outer flow may swirl around the fuel rods several times. The differential equations describing the temperatures at the four nodes are as follows:

$$(MC_p)_{fl} \frac{dT_{fl}}{dt} = P_{fl} n - (UA)_{fl} (T_{fl} - T_{cl}) - (UA)_{tr} (T_{fl} - T_{f2}) \qquad \ldots(1)$$

$$(MC_p)_{f2} \frac{dT_{f2}}{dt} = P_{f2}n - (UA)_{f2}(T_{f2} - T_{c2}) + (UA)_{tr}(T_{f1} - T_{f2}) \quad \ldots(2)$$

$$(MC_p)_{c1} \frac{dT_{c1}}{dt} = (UA)_{f1}(T_{f1} - T_{c1}) - (wC_p)_{c1}(T_{out1} - T_{in}) - (wC_p)_c(M_x)(T_{c1} - T_{c2}) \quad \ldots(3)$$

$$(MC_p)_{c2} \frac{dT_{c2}}{dt} = (UA)_{f2}(T_{f2} - T_{c2}) - (wC_p)_{c2}(T_{out2} - T_{in}) + (wC_p)_c(M_x)(T_{c1} - T_{c2}) \quad \ldots(4)$$

Here the symbols have standard definitions, and Subscripts 1, 2, and tr refer to outer and inner regions and transport between them, respectively. The distinguishing feature of these equations is the last term in Equations 3 and 4. As the fuel rods bow with increasing temperature, the "mixing fraction," M_x, increases and thereby increases the inner coolant temperature. As T_{c2} increases, fuel rod bowing tends to decrease; thus, the restoring force necessary for oscillation is provided.

Fuel rod bowing is determined by the temperature difference between the inner and outer cladding, since the fuel is in the form of 6-in.-long slugs. Detailed calculations of the temperature distribution show that the cladding temperature is well represented by:

$$T_{clad} = (1/3)T_f + (2/3)T_c \quad .$$

Thus, the difference between outside and inside cladding temperature is:

$$(\Delta T)_{clad} = 1/3\,(T_{f1} - T_{f2} + 2T_{c1} - 2T_{c2}) \quad . \quad \ldots(5)$$

If d is the peak deflection of a rod per °F of $(\Delta T)_{clad}$, then the average bowing is:

$$\delta\bar{r} = \frac{d}{6}(T_{f1} - T_{f2} + 2T_{c1} - 2T_{c2}) \quad . \quad \ldots(6)$$

As the rods bow, mixing flow increases. The change is assumed to be proportional to the average change in the spacing between the rods. This is expressed as:

$$M_x = M_{x_{oo}} \left(1 + \frac{\delta M_x}{M_{x_{oo}}}\right) = M_{x_{oo}} \left(1 + \frac{2\pi \delta \bar{r}}{5 b_o}\right) = M_{x_{oo}} (1 + a\, \delta \bar{r}) \ , \qquad \ldots(7)$$

where b_o is the initial spacing between the 5 rods, and M_{xoo} is the fraction of the total flow which flows between the rods at zero power. Since b_o = 90 mils,

$$M_x = M_{x_{oo}} (1 + 0.014\, \delta \bar{r}) \ . \qquad \ldots(8)$$

The flows inside and outside the cluster also change with bowing. This change may be expressed as the change in average flow volume in each region:

$$\frac{\delta w_1}{w_{1_{oo}}} = -\frac{\delta \bar{r}}{250 - r_o} \ ,$$

where r_o is the zero power deflection from an original spacing of 250 mils. The regional flows become:

$$w_1 = w_{1_{oo}} \left(1 - \frac{\delta \bar{r}}{250 - r_o}\right) \ , \qquad \ldots(9)$$

and

$$w_2 = w_{2_{oo}} \left[1 + \left(\frac{\delta \bar{r}}{250 - r_o}\right)\left(\frac{w_{1_{oo}}}{w_{2_{oo}}}\right)\right] \ , \qquad \ldots(10)$$

where $w_{1_{oo}}$ and $w_{2_{oo}}$ are the respective regional flows at zero power. The fuel rods deflect due to normal "sagging," since the lower ends of the rods are fixed. This effect, as measured directly and calculated from zero-power criticality measurements with a single constrained fuel cluster, is about 80 mils peak at zero power, or 40 mils average.[7] Since $w_{1_{oo}}/w_{2_{oo}}$ = 3 for the no-bowing case, substitution in Equations 9 and 10 gives:

$$w_{1_{oo}} = 0.63w, \text{ and } w_{2_{oo}} = 0.37w \ .$$

Therefore,

$$w_1 = 0.63w \left(1 - \frac{\delta \bar{r}}{210}\right) = 0.63w \, (1 - K_1' \, \delta \bar{r}) \quad , \qquad \ldots(11)$$

and

$$w_2 = 0.37w \left[1 + \frac{\delta \bar{r}}{210} \, (1.7)\right] = 0.37w \, (1 + K_2' \, \delta \bar{r}) \quad . \qquad \ldots(12)$$

Finally, assuming T_i constant, and redefining all temperatures as the excess above T_i (e.g., $T_f = T_f - T_i$), Equations 1 through 4 are written:

$$\tau_{f1} \frac{dT_{f1}}{dt} = K_{f1} n - (T_{f1} - T_{c1}) - K_f' \, (T_{f1} - T_{f2}) \qquad \ldots(13)$$

$$\tau_{f2} \frac{dT_{f2}}{dt} = K_{f2} n - (T_{f2} - T_{c2}) + K_f' \, (T_{f1} - T_{f2}) \qquad \ldots(14)$$

$$\tau_{c1} \frac{dT_{c1}}{dt} = (T_{f1} - T_{c1}) - 2K_{c1} [w_1] (T_{c1}) - K_c w [M_x] (T_{c1} - T_{c2}) \qquad \ldots(15)$$

$$\tau_{c2} \frac{dT_{c2}}{dt} = (T_{f2} - T_{c2}) - 2K_{c2} [w_2] (T_{c2}) + K_c w [M_x] (T_{c1} - T_{c2}) \quad , \ldots(16)$$

since $T_{out} = 2T_c$. The quantities in brackets are those which vary with bowing. The constants are:

$$\tau_{f1} = \tau_{f2} = \frac{(MC_p)_f}{(UA)_{fc}} \; ; \; K_f' = \frac{(UA)_{tr}}{(UA)_{fc}} \, ,$$

$$K_{f1} = \frac{P_{f1}}{(UA)_{fc}} ; \; K_{f2} = \frac{P_{f2}}{(UA)_{fc}} \quad ,$$

$$\tau_{c1} = \frac{(MC_p)_{c1}}{(UA)_{fc}} \; ; \; \tau_{c2} = \frac{(MC_p)_{c2}}{(UA)_{fc}} \quad ,$$

and

$$K_{c1} = K_{c2} = K_c = \frac{(C_p)_c}{(UA)_{fc}} \quad ,$$

where

$$(UA)_{fc} = (UA)_{f1} = (UA)_{f2} \quad .$$

Thus, Equations 6, 8, and 11 through 16 define the mathematical "mixing model." In the following section, these equations are solved on an analog computer in order to examine the power coefficient of the SRE.

III. POWER COEFFICIENT

In order to study the SRE Core II power coefficient and to provide steady-state conditions for study of the flux and temperature oscillations, the foregoing nonlinear differential equations were solved on an analog computer. Although the analog circuitry is not included here, a block diagram is shown in Figure 5.

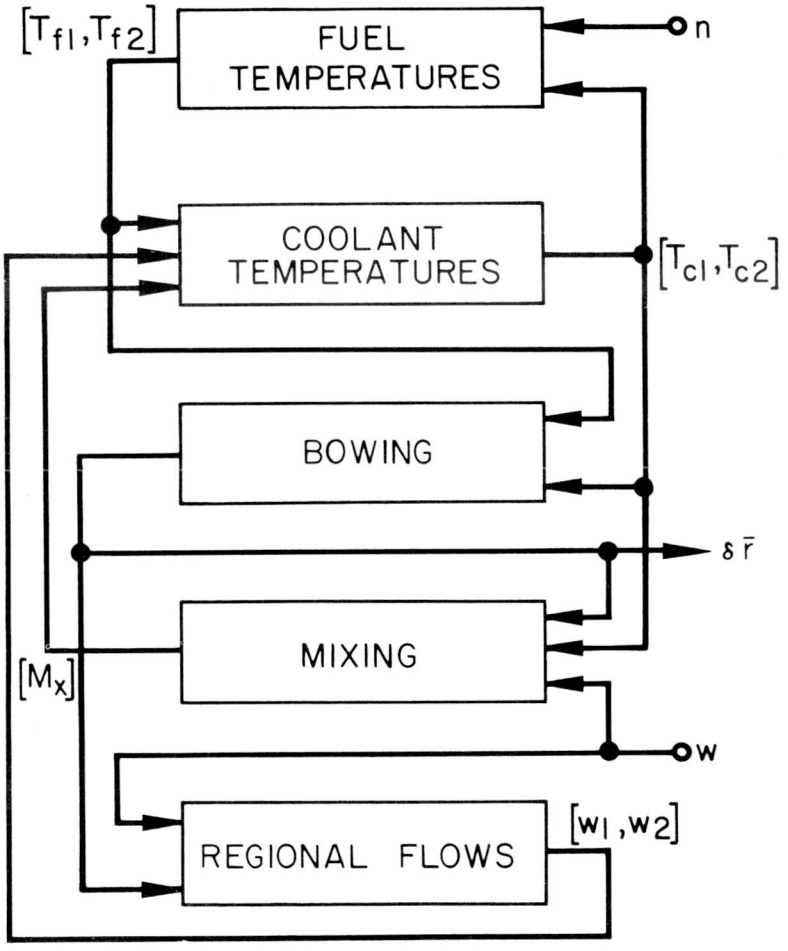

7602-4619

Figure 5. Block Diagram, Mixing Model

As previously stated, outward bowing of the fuel rods was the cause of the positive prompt power coefficient. Therefore, the analog was used to solve for the bowing, $\delta\bar{r}$, as a function of power. Assuming a constant coefficient of reactivity for bowing, the prompt power coefficient then becomes the slope of the bowing vs power curve. The core parameters used in calculating the constants of the model equations were the best values available. The parameters concerning

bowing and mixing were subject to some question, and were varied widely on the analog. Since the results outlined in this section were achieved with several sets of bowing parameters, parameter values will not be presented here. However, the character of the results is clear.

Using reasonable parameter values, the computed prompt power coefficient compared extremely well with the measured results (Figure 6), and the tendency for the coefficient to "flatten out" as the core ΔT increased was reproduced. This behavior was confirmed for different flow rates, and implied that bowing tended toward a linear function of power as power increased. In the model, as power rises and the fuel rods begin to bow, the mixing from outer to inner channels increases and the outer region flow decreases. The former effect decreases T_{c1} (hence, ΔT_c), while the latter increases it. At first, the regional flow effect predominates, and ΔT_c rises sharply; but as the mixing effect increases, the rate of change of ΔT_c approaches linearity.

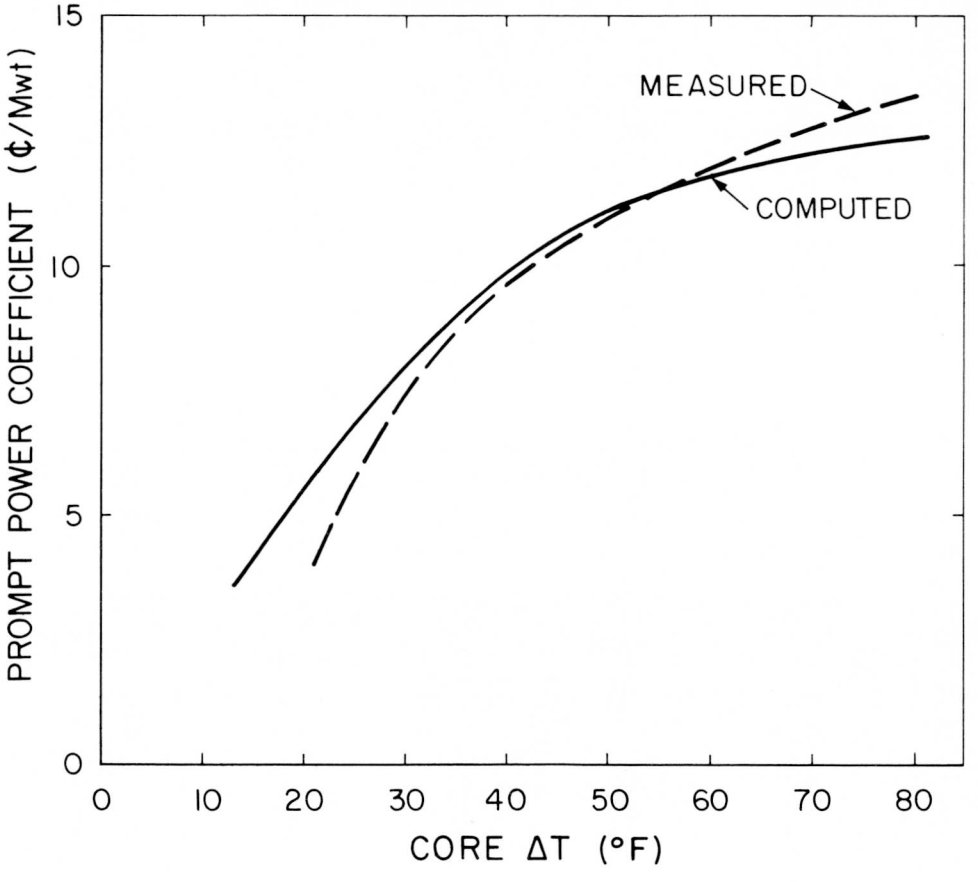

Figure 6. Prompt Power Coefficient, Measured and Calculated

In addition, because of the sharp rise in ΔT_c due to regional flow change with bowing, δ_r^- rises sharply, exhibiting an exponential-like behavior (Figure 7) at lower ΔT's. This effect substantiates previous assumptions of an exponential flux or bowing character in analyzing ramp measurements,[2] and provides the sharp increase of the power coefficient at low core ΔT's (Figure 6).

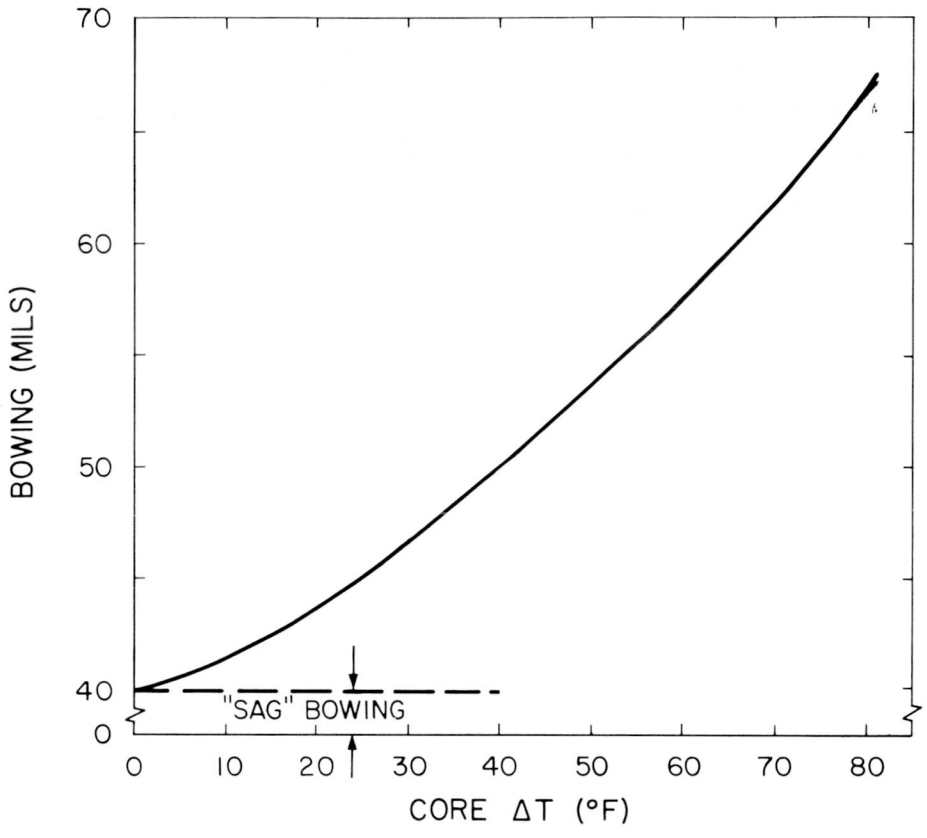

Figure 7. Calculated Fuel Rod Bowing as a Function of Core ΔT

In the next section, the oscillating character of the model is examined, using core parameters obtained during these static studies. Note that the model as programmed on the analog computer showed tendencies to oscillate, using various sets of reasonable bowing parameters.

IV. FLUX OSCILLATIONS

Although the analog computer was required for the above work in examining the nonlinear nature of the power coefficient, for analysis of flux oscillations, it is possible to linearize the equations and solve them analytically. The analog computer results will then be used to determine the equilibrium conditions for the linearized model.

Trial and error attempts at an analytical solution of the equations showed that the simplest and most useful solution is obtained by solving for the difference in the inner and outer channel coolant temperature. For simplicity it was assumed that the difference in temperature across the cladding is determined only by the difference in coolant temperature; the effect of fuel temperature on bowing is thus neglected.

The linearized equations for fuel temperature, from Equations 13 and 14, yield:

$$\delta T_{f1} - \delta T_{f2} = \frac{\delta n(K_{f1} - K_{f2}) + (\delta T_{c1} - \delta T_{c2})}{\tau_f s + 1} \quad . \qquad \ldots(17)$$

The coolant equations, when Equations 6, 8, 11, and 12 are inserted into Equations 15 and 16, become in the linearized form:

$$\tau_{c1} s\ \delta T_{c1} = (\delta T_{f1} - \delta T_{c1}) - 2 K_c w_{1_o} \left[-K_1' d\ T_{c1_o} (\delta T_{c1} - \delta T_{c2}) + \delta T_{c1}\right]$$

$$- K_c w_o \left[M_{x_o} + M_{x_{oo}} ad\ \Delta T_{c_o}\right] (\delta T_{c1} - \delta T_{c2}) \qquad \ldots(18)$$

$$\tau_{c2} s\ \delta T_{c2} = (\delta T_{f2} - \delta T_{c2}) - 2 K_c w_{2_o} \left[K_2' d\ T_{c2_o} (\delta T_{c1} - \delta T_{c2}) + \delta T_{c2}\right]$$

$$+ K_c w_o \left[M_{x_o} + M_{x_{oo}} ad\ \Delta T_{c_o}\right] (\delta T_{c1} - \delta T_{c2}) \ , \qquad \ldots(19)$$

where terms with subscript "o" refer to equilibrium at-power conditions.

One parameter not present in the previous analysis must be added: a lag term associated with changes in mixing flow and regional flow. Although the bowing of the fuel rod proceeds essentially simultaneously with changes in temperature, there is a transport lag associated with changes in the flow between the rods, and the consequent change in regional flow. This lag is about 1 sec (because of the spiral flow path) at 650 gpm, which is the flow which will be used for this analysis. However, Storrer[8] showed that a temperature wave is transported more slowly than the coolant velocity, because the wave must also change the temperature of the fuel. It is not clear how this should be treated in the case of flow between fuel rods; but based on Storrer's expressions, it was estimated that the temperature travels a factor of 2 slower than the coolant. For simplicity, this was treated as a time lag; i.e., $(\tau_x s + 1)^{-1}$ instead of a transport lag.

From Equations 6 and 7,

$$M_{x_o} = M_{x_{oo}} + ad\ \Delta T_{c_o} ,$$

where ΔT_{c_o} is determined from the analysis with the analog computer.
It is convenient to define

$$P = \frac{\Delta T_{c_o}}{\Delta T_{core}} ,$$

and also to assume

$$T_{c1_o} = T_{c2_o} = (1/2)\Delta T_{core} ,$$

which the nonlinear analysis showed to be reasonably accurate, for the power and flow rates used here.

Including these factors in Equations 18 and 19, partially solving each equation, and subtracting 19 from 18:

$$\left[\tau_{c1}\, s + (1 + 2\, K_c w_{1_o})\right] (\delta T_{c1} - \delta T_{c2}) = \delta T_{f1} - \delta T_{f2}$$

$$+ \frac{2K_c d\, (\delta T_{c1} - \delta T_{c2})\, (w_{1_o} K_1' T_{c1_o} + w_{2_o} K_2' T_{c2_o})}{\tau_x\, s + 1}$$

$$- \frac{2K_c w_o M_{x_{oo}}}{\tau_x\, s + 1} \left[1 + 2ad\, \Delta T_{c_o}\right] (\delta T_{c1} - \delta T_{c2}) \ , \qquad \ldots(20)$$

where it has been assumed (again based on the analog results):

$$\tau_{c2} s + (1 + 2\, K_c w_{2_o}) = \tau_{c1}\, s + (1 + 2\, K_c w_{1_o}) \ .$$

Use of Equation 17 now gives the required solution. It is convenient to write this in the form of a feedback system, to permit the use of root-locus analysis rather than a direct solution of the equation:

$$(\delta T_{c1} - \delta T_{c2}) = \frac{\delta n (K_{f1} - K_{f2})}{\tau_f\, s + (1 + 2K_f')} \quad \frac{1}{\tau_{c1}\, \tau_f} \quad G_c(s) - \tau_f K_c' H_c(s)\, (\delta T_{c1} - \delta T_{c2}) \ , \qquad \ldots(21)$$

where

$$G_c(s) = \frac{s + \dfrac{(1 + 2\, K_f')}{\tau_f}}{s^2 + \left[\dfrac{(1 + 2K_f')}{\tau_f} + \dfrac{(1 + 2K_c\, w_{1_o})}{\tau_{c1}}\right] s + \left[\dfrac{(1 + 2K_f')\, (1 + 2K_c\, w_{1_o}) - 1}{\tau_f\ \tau_{c1}}\right]} \qquad \ldots(22)$$

$$H_c(s) = \frac{1}{s + 1/\tau_x} \qquad \ldots(23)$$

$$K'_c = \frac{2K_c w_o M_{x_{oo}}}{\tau_{c1}\tau_x} + \frac{2K_c w_o d}{\tau_{c1}\tau_x}\left[2a M_{x_{oo}} P - (1/2)\left(\frac{w_{1_o}}{w_o}K'_1 + \frac{w_{2_o}}{w_o}K'_2\right)\right]\Delta T_{core} \quad , \qquad \ldots(24)$$

and the factors are in the form required for root-locus analysis.

The roots of the denominator of G(s) are always real and negative for conditions in the SRE. Using parameters consistent with those discussed in the previous section, a root-locus plot for this system is shown in Figure 8, plotted positive values of K (negative feedback). From this plot, the following interesting conclusions can be reached.

a) The system exhibits damped oscillations for gains greater than a certain critical value. For conditions in the SRE, the gain is always greater than this value.

b) Without the lag associated with the transport time for mixing, no oscillations could exist since the roots would always lie on the negative real axis.

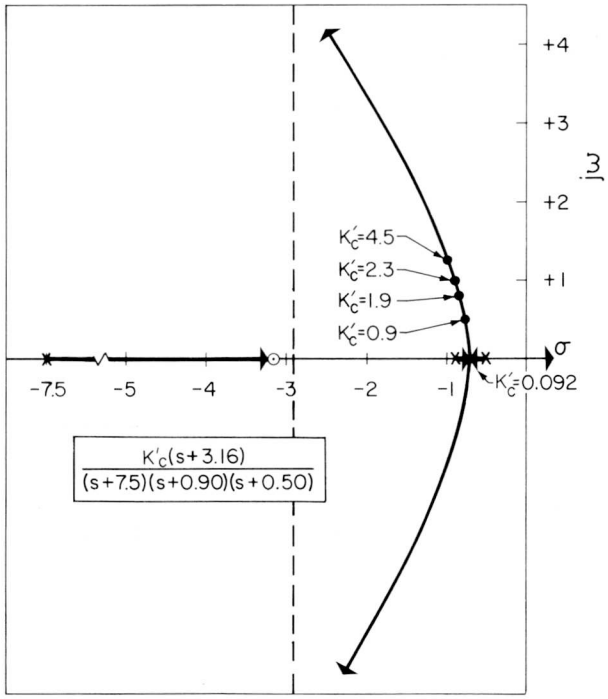

7602-4614

Figure 8. Root Locus of Coolant Temperature Difference

c) In the expression for the gain, Equation 24, the coefficient of ΔT_{core} can be either positive or negative. Since for negative values of gain the roots would all lie on the real axis and one root would become positive, a reasonable requirement on the parameters involved is that this coefficient be negative. This coefficient represents the interplay between changes in regional flow, which tend to increase the bowing, and changes in mixing flow which tend to limit the bowing. If the change in regional flow is sufficiently effective, no stable condition will exist until the process channel physically restrains the rods. The requirement that the coefficient of ΔT_{core} be negative thus requires that the mixing flow be more effective than changes in regional flow.

d) No great significance should be attached to the exact position of the poles in Figure 8, since this diagram corresponds to only one of many possible (and reasonable) sets of parameters. However, for conditions in the SRE the gain lies in the range of 1 to 6, and the associated frequency of oscillation agrees quite well with the measured value (Figure 3).

Before further conclusions are reached, it is necessary to include the effects of kinetics. A control system diagram for this is shown in Figure 9, using linearized, one delay-group kinetics. Notice that since root-locus assumes unity feedback, the feedback term existing in the coolant temperature loop must be brought into the forward transfer function and then compensated for, outside the loop. Since the gain around this inner loop is in the feedback, it does not affect the closed loop gain, but only the position of the poles.

The open loop transfer function for the system shown in Figure 9 is:

$$KG(s)H(s) = \frac{n_o \beta (K_{f1} - K_{f2})}{\ell} \frac{(\alpha_B)_d}{\tau_f \tau_{c1}} \frac{(s + 0.1)(s + 0.5)}{s(s + 14)(s + 7)(s + a_1)(s + a_2)} , \quad \ldots (25)$$

where a_1 and a_2 are the complex poles determined from the above analysis, and α_B is the bowing coefficient of reactivity.

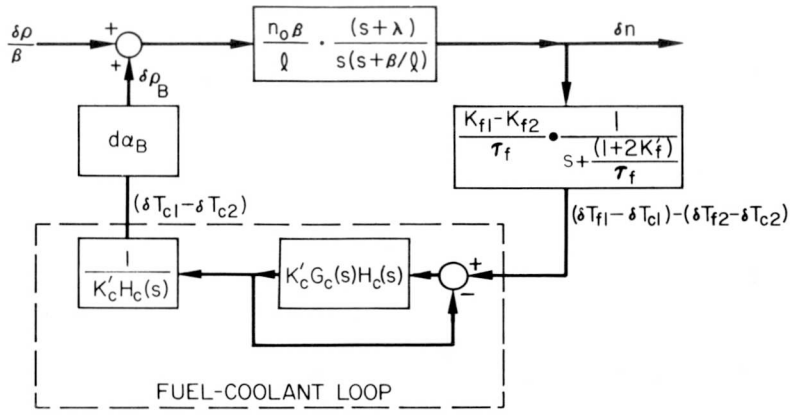

7602-4615

Figure 9. Control Diagram of Kinetics With Feedback

The root-locus for this system is shown in Figure 10. This is plotted for negative values of gain since the feedback is positive due to the positive bowing coefficient. No feedback due to the negative Doppler coefficient is included, but this would have little effect on the general character of the plot because it is much smaller than the bowing coefficient.

This root-locus indicates that the oscillations are always damped. However, by somewhat changing the parameters in the fuel-coolant loop it is possible to obtain the plot shown in Figure 11 where the locus crosses the imaginery axis. Thus, sustained oscillations may be explained either by assuming parameters such that the poles always lie exactly on the imaginery axis, or by assuming damped oscillations continuously excited by an undefined tickling function. Experimental data supports the second hypothesis for the following reasons.

a) Temperature oscillations in the fuel channel were observed to start and stop at random. This implies some unknown effect which supports the oscillations under certain conditions.

b) According to the plot shown in Figure 11, if sustained oscillations exist at a particular gain (i.e., power level), then a slightly higher gain should cause divergent oscillations. However, extensive measurements over a wide range of powers and flow rates showed no divergence.

c) A system which exhibits natural undamped oscillations will become divergent when forced with an oscillating input of the same frequency. Measurements of the transfer function used an oscillating reactivity input, but no

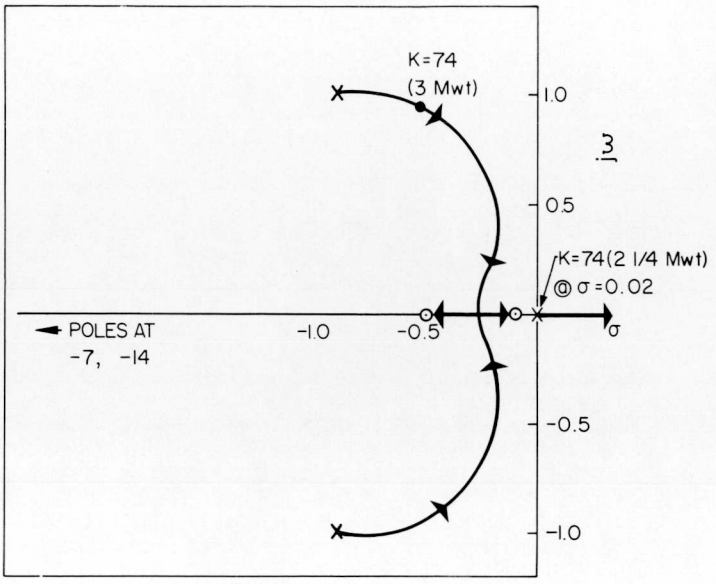

7602-4616

Figure 10. Root Locus of Kinetics and Feedback, Negative Gain (Positive Feedback)

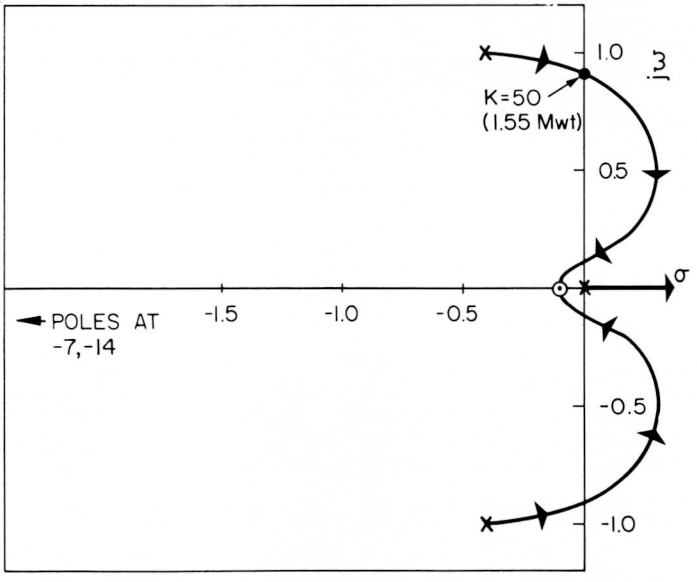

7602-4617

Figure 11. Root Locus of Kinetics and Feedback Showing Undamped Oscillations

divergence was observed in spite of extensive, and repeated measurements at very small frequency increments.

Although the experimental data thus indicate the existence of a tickling function which is effective in sustaining the oscillations under certain conditions, no firm conclusions regarding the nature of this function have been reached. One interesting suggestion is based on the possibility of unstable flow in the channel. Rough calculations of the flow characteristics inside the cluster indicate that the Reynold's number may be close to the critical region between laminar and turbulent flow. Changes in the coolant velocity, hydraulic diameter, or kinematic viscosity could cause the flow to lie in this criticality region. Under these conditions the flow will exhibit pulses with a frequency proportional to the flow velocity,[9] and these pulses could provide the necessary triggering.

One additional hypothesis should be mentioned in passing. Since Figure 11 demonstrates the possibility of positive roots, the undamped oscillations may be restrained by a limit cycle. The simple linear analysis herein does not exclude such a possibility, and a thorough nonlinear examination of the model may verify it. Such work is beyond the scope of this report.

Using the above linear analysis, it is possible to investigate the dependence of the oscillations on power and flow. From Equation 24, the gain of the fuel-coolant loop can be written:

$$K_C' = Aw_o + Bn_o \quad , \qquad \ldots(26)$$

so the location of the complex poles of this loop depends both on power and flow. Thus, in the root-locus for the complete system it is permissible to use only those power levels which are consistent with Equation 26. To investigate the changes in the oscillations with power and flow the following three sets of parameters were used.

a) Power = 3.2 Mw, flow rate = 650 gpm, $K_C' = 1.9$, $K = 100$

b) Power = 3.2 Mw, flow rate = 950 gpm, $K_C' = 2.3$, $K = 100$

c) Power = 4.5 Mw, flow rate = 650 gpm, $K_C' = 2.3$, $K = 150$

The location of the corresponding poles of the complete system are shown in Figure 12. Increasing the flow rate at constant power increases the frequency

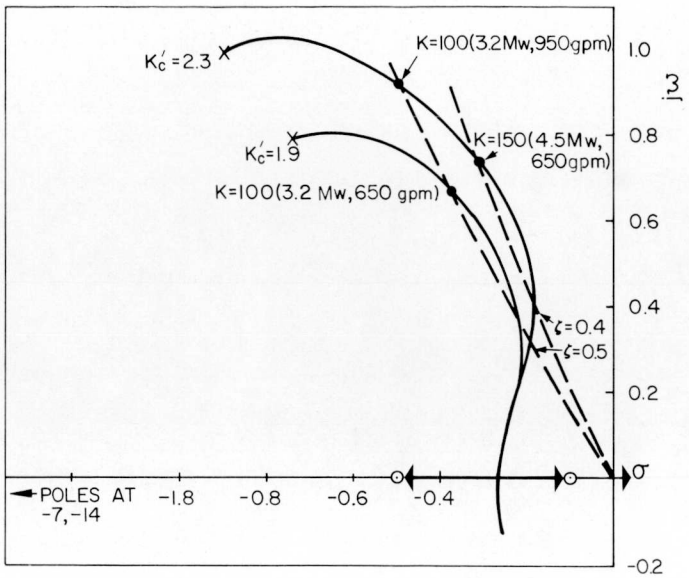

7602-4623

Figure 12. Expanded Root Locus Plot Showing Poles At Different Power and Flow

of the oscillations, but leaves the damping factor unchanged. Increasing the power level at constant flow, however, decreases the damping factor but leaves the frequency essentially unchanged. Both of these results are in excellent agreement with experimental data shown in Figure 3. Again note that the exact location of the poles, and particularly the damping factor, can be varied considerably within the credible range of the various parameters.

It is not clear whether the change in the damping factor predicted by the above analysis is sufficient to cause the strong dependence of the amplitude of the oscillations on power level (ΔT_{core}). However, if rapid changes in flow represent the tickling function, then these pulses would produce corresponding temperature pulses proportional to ΔT_{core}. The change in the damping factor with power level would then cause the upward curvature in the curve of amplitude vs delta T shown in Figure 3.

V. CALCULATION OF TRANSFER FUNCTION

Based on the root-locus plot shown in Figure 10, the closed loop transfer function of the system in Figure 9 can be calculated. Again it is necessary to compensate for the nonunity nature of the feedback loop. Using the poles corresponding to K = 37 (which is about 3 Mwt), the transfer function is found to be approximately:

$$\frac{C(s)}{R(s)} = \frac{n_o \beta}{\ell} \frac{(s + 0.1)(s^2 + 2s + 2)}{(s - 0.01)(s + 14)(s^2 + 1.5s + 1.56)} \quad . \qquad \ldots(27)$$

A Bode plot of this function is shown in Figure 13. Comparison of this with the measured transfer function at similar reactor conditions (Figure 4) reveals agreement in the following areas.

a) A general rise in gain occurs in the region of 0.1 to 0.3 cps, and a dip in the phase angle occurs at a slightly higher frequency.

b) The at-power gain at low frequencies (below 0.1 cps), lies above that at zero power, and the at-power phase lies below the zero power results. This effect is due to the additional feedback of the fuel-coolant loop, H_c. Above the break frequency of the coolant transport lag (about f = 0.17 cps), $|H_c|$ falls rapidly, and the system gain returns to normal. Elimination of the bowing feedback (by wire restraints) also brought the low frequency system response back to normal by making d = 0.

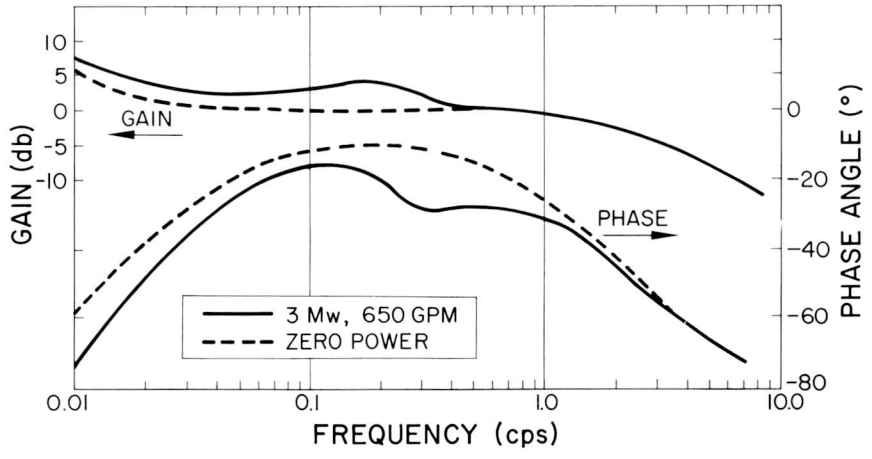

7602-4621

Figure 13. Calculated Transfer Function

The general features of the measured transfer function are thus exactly duplicated by this model, with only the sharp resonance peaks remaining to be explained. These are probably the result of interference of the sustained flux oscillations with the measurement, as shown below.

The spectral density of a function x(t) may be defined as:[10]

$$S(\omega) \equiv \lim_{T \to \infty} \frac{1}{2T} \left| X_T(j\omega) \right|^2 , \qquad \ldots(28)$$

where

$$X_T(j\omega) = \int_{-T}^{T} x(t) e^{-j\omega t} dt . \qquad \ldots(29)$$

Measurement of $S(\omega)$ can be performed by neglecting the limit process in equation 28, so that for a measuring time T:

$$S(\omega) \approx \frac{1}{T} \left\{ \left[\int_o^T x(t) \cos \omega t \, dt \right]^2 + \left[\int_o^T x(t) \sin \omega t \, dt \right]^2 \right\} . \qquad \ldots(30)$$

The operations indicated by Equation 30 are also used in oscillation measurements at the SRE[6] to eliminate higher harmonics associated with the nonsinusoidal reactivity input. Thus, the measured transfer function also includes the power spectral density of the reactor noise. This is usually very much smaller than the forced oscillations, and produces no significant effect. The sustained oscillations, however, were about the same size as the forced oscillations, and could thus strongly perturb the measurement at certain frequencies, producing apparent spikes in the transfer function.

Griffin and Randall have suggested[4] that the exact character of the oscillations could be studied by comparison of the effect which they produce on oscillation measurements and noise analysis. However, investigation has shown that some ambiguity arises in this analysis. It is hoped that the present model will assist in resolving this difficulty, so that this technique can be used to study further the undefined tickling function.

VI. CONCLUSION

The model presented in this paper differs from the usual treatment of fuel-coolant temperature response by including a mixing flow between the rods, which tends to equalize the temperatures inside and outside the rods. Bowing of the fuel rods changed the amount of mixing flow, and also the ratio of flow inside and outside the cluster. As shown in this paper, these flow changes caused:

a) the dependence of the prompt power coefficient on the power level, which caused the reactor to be relatively stable at low power and caused loss of self-regulation at higher power;

b) the possibility of oscillations in the temperature, which produced flux oscillations through bowing effects;

c) the approximate frequency of these oscillations, and the dependence of the frequency on solely the flow rate; and

d) the nature of the reactor transfer function.

The existence of sustained oscillations was made possible by an undefined tickling function, and the hypothesis that this function is associated with coolant flow explains the dependence of the amplitude of the oscillations on the core delta T. In addition, the model describes the results of corrective action, in which constraining the fuel clusters produced the return of self-regulation and the disappearance of oscillations.

The model used in this analysis has several deficiencies, particularly in the lack of any axial spatial dependence, and in the over-simplified treatment of the hydraulics in the channel. This approach produces a certain artificiality in some of the parameters, making it impossible to calculate them accurately from first principles. However, in view of the success of the present analysis, there is no apparent justification for a more complicated treatment.

Throughout the analysis, reasonable values of the various parameters involved were used, but no attempt was made to determine a best set of values. In principle, this could be done by forcing the model to give the best possible duplication of the exact experimental results. This was not necessary, however,

for the purpose of this investigation, which was to gain a physical understanding of the causes of the above behavior, so that future fuel element designs will be free of such phenomena. To accomplish this purpose, the following recommendations are made.

a) Subject proposed fuel elements to a thorough hydraulic study, experimentally and analytically, being certain that Reynold's numbers are well above the critical region.

b) Restrain fuel elements from all forms of motion within a fuel channel.

NOMENCLATURE

M = mass (fuel or coolant)

C_p = specific heat (fuel or coolant)

P_{f1}, P_{f2} = heat generation fraction, fuel regions 1 and 2

UA = overall heat transfer coefficient times area

n = reactor power level

w = coolant flow

M_x = "mixing fraction," portion of total coolant flow flowing from Region 1 to 2

$M_{x_{oo}}$ = mixing at zero power

M_{x_o} = mixing at equilibrium power

a = change in mixing with bowing

d = temperature coefficient of bowing

$\delta\bar{r}$ = bowing from zero power

K_1', K_2' = change in regional flows due to bowing

τ_f = fuel temperature time constant

τ_{c1}, τ_{c2} = coolant temperature time constants

K_{f1}, K_{f2} = $P_f/(UA)_{fc}$ for each fuel region

$K_f' = (UA)_{tr}/(UA)_{fc}$, conduction between fuel regions

$K_c = (C_p)_c/(UA)_{fc}$ for coolant

ΔT_c = temperature difference between coolant regions

δT = change in temperature from equilibrium

s = Laplacian operator

K_c' = open-loop fuel-coolant gain

τ_x = transport lag time constant

P = ratio of coolant ΔT to core ΔT

α_B = bowing coefficient of reactivity

K = open-loop system gain

Subscripts

1, 2 = "outer" and "inner" regions, respectively

tr = transport between regions

oo = at zero power

o = at equilibrium power

fc = fuel-to-coolant

REFERENCES

1. H. F. Donohue and R. W. Keaten, "Fuel Rod Bowing In The SRE," Trans Am. Nuclear Society 5, 172 (June 1962) – also published as NAA-SR-6878 (June 1962)

2. C. W. Griffin, "Analysis of the Sodium Reactor Experiment Prompt Power Coefficient," Nuclear Science and Engineering 14, 304 (November 1962)

3. R. W. Woodruff, C. W. Griffin and R. W. Keaten, "Detecting and Eliminating Fuel Rod Bowing In The SRE," NAA-SR-7705 (February 1963)

4. C. W. Griffin and R. L. Randall, "At-Power, Low-Frequency Reactor Power-Spectrum Measurements and Comparison with Oscillation Measurements," Nuclear Science and Engineering 15, 131 (February 1963)

5. F. L. Fillmore and J. R. Burr, "Monte Carlo Circulations Using the RBUMC Code," AMTD-194 (February 1963)

6. C. W. Griffin and R. W. Keaten, "Oscillation Measurements In The SRE," NAA-SR-7264 (to be published)

7. E. N. Pearson, unpublished data

8. Fred Storrer, "Temperature Response To Power, Inlet Coolant Temperature and Flow Transients in Solid Fuel Reactors," APDA-132 (June 1959)

9. Harold Etherington, Nuclear Engineering Handbook Section 9-2 (McGraw-Hill Book Co., New York, 1958)

10. V. V. Solodovnikov, Introduction To The Statistical Dynamics of Automatic Control (Dover Publications, Inc., New York, 1960)